RSC Advances

ROYAL SOCIETY OF CHEMISTRY

www.rsc.org/advances

A computational investigation on the substituent effect on the chemo- and stereoselectivity of crossed intermolecular radical anion [2+2] cycloadditions of enones

Chenchen Guo [a], Huiqun Wang [a], Bo-Zhen Chen [a,*], Zhiyuan Tian [a]

[a] *School of Chemistry and Chemical Engineering, University of Chinese Academy of Sciences, No. 19A, YuQuan Road, Beijing 100049, P. R. China*

Abstract

Density functional theory calculations have proven the polar nature of the crossed intermolecular radical anion cycloadditions of various enones. The substituent effects on the chemo- and stereoselectivity of the cycloadditions have been elucidated. The electronic structures of the substituents strongly influence the formation of the radical anion and the reactivity of cycloaddition. The amino and nitryl substituents are both unfavorable for the cycloaddition. The cycloaddition is sensitive to the substituents on the C atoms which form σ bond in the first cycloaddition step by both steric hindrance and electronic effect. To improve the chemoselectivity, one of these C atoms should be unsubstituted. The stereoselectivity mainly caused by the difference in steric interaction between the trans and cis transition states is benefited by the bulky substituents on the carbonyl.

Keywords: DFT; [2+2] cycloaddition; chemoselectivity; stereoselectivity; substituent effect.

* Corresponding author. Tel.: +86 10 88256129; Fax: +86 10 88256092.

E-mail address: bozhenchen@hotmail.com (B.-Z. Chen).

1. Introduction

The cyclobutane is a key structure in various bioactive natural products.[1,2] In the last century, [2+2] cycloadditions of enones promoted by UV irradiation were recognized as an efficient method for construction of strained four-membered rings.[3-7] However, this method is limited to the intermolecular cycloadditions of enones, as the enones undergo rapid cis-trans isomerization under UV irradiation, which is an energy wasting progress dramatically diminishing the efficiency of productive cyclobutane. Additionally, the cis-trans isomerization of the enone reactants, leading to various cyclobutane products with different stereo structures, is very unfavorable for using in pharmaceutical synthesis.

The intermolecular radical cation cycloaddition of styrenes has been found to have low activation barrier and excellent stereoselectivity.[8-11] Thereafter, a variety of intramolecular radical anion cycloadditions of bis(enones) were carried out using electrocatalysis[12] and chemically induced[13] methods. However, the development of the intermolecular radical anion cycloaddition is limited by the initiation methods. Recently, the T. P. Yoon's laboratory have reported that $Ru(bipy)_3^{2+}$ serves as an excellent visible light photocatalyst for initiating the inter-/intramolecular anion/cation [2+2] cycloaddition,[14-17] representing a considerable advance in construction of cyclobutane-containing structures. In our previous studies, we have investigated the intramolecular cycloadditions of bis(enones) and bis(styrenes) and the intermolecular cycloaddition between phenyl vinyl sulfone and enone by theoretical methods.[18-21] The investigation gave an insight into the origin of the stereoselectivity of intramolecular cycloadditions and the regioselectivity of intermolecular cycloaddition. However, the origin of the chemo- and stereoselectivity of intermolecular cycloaddition is still unclear.

The experimental investigation of the intermolecular cycloadditions of enones (reactions 1-3 and 6-9 shown in Table 1(b)) showed that the substituents had a dramatic effect on the reactivity and stereoselectivity of the cycloaddition.[15] Reactions 1-3 and 6 show good yield and excellent stereoselectivity to form the trans products.

The yields of reactions 7 and 8 are relative low, but the stereoselectivity was kept. The stereoselectivity of reaction 9 substituted by methoxyl on carbonyl is not so excellent as other reactions. To avoid the undesired homodimerization, the researchers used two dissimilar enone substrates in all the reactions. One of the reactants must be aryl enone to initiate the radical anion reaction. The other is acting as a Michael acceptor. All the reactions except reaction 8 gave excellent chemoselectivity to form the crossed cycloaddition products. However, in reaction 8, the yield of the homodimerization product of the aryl enone is higher than that of the crossed cycloaddition products. In this paper, we not only calculated these above reactions 1-3, and 6-9, but also designed and calculated reactions 4, 5, and 10-16 (see Table 1(b)), to investigate the substituent effect on the chemo- and stereoselectivity of the intermolecular cycloaddition. We hope that our investigations can provide important information for further designing new novel intermolecular [2+2] cycloadditions.

2. **Computational methods**

The geometries of all stationary points, including the minimum energy structures and saddle points, were optimized at the DFT B3LYP[22-24] level with the 6-311+(d,p) basis set. The chosen basis set including diffuse and polarization functions are usually important in the geometry optimizations for radical anions[25].

Frequency analysis calculations at the B3LYP level at 298 K were performed to confirm each stationary point along the reaction pathway to be either a minimum (no imaginary frequencies) or a transition-state (only one imaginary frequency). The intrinsic reaction coordinate (**IRC**)[26-28] pathways have been traced to confirm whether the transition state connects the reactant, intermediate, or product. The energies presented in this paper were corrected with zero-point energies (ZPEs) calculated at the B3LYP/6-311+G(d,p) level. Gibbs free energies and enthalpies in gas phase at 298 K and 1 atm were calculated at the same level. The single-point solvation Gibbs free energies were calculated by using SMD solvation model in CH_3CN solvent (used in the experiment) at the same level as well.[29]

All of the quantum chemical calculations were performed using the Gaussian 09 program.[30] The $<S^2>$ values for the doublet states of all the reactants, transition states, intermediates, and products along the reaction pathways at the

(U)B3LYP/6-311+G(d,p) level were less than 0.78, where the double state is expected to be 0.75.

3. Results and Discussion

The experimental investigation of the intermolecular cycloadditions of enones (reactions 1-3 and 6-9) shows that only the cyclobutane products with carbonyls in ortho position are observed, indicating the excellent regioselectivity. In the previous study of the cycloaddition between phenyl vinyl sulfone and enone,[21] the phenyl sulfonyl and carbonyl of the dominating product are in ortho position as well, which is attributed to the p-π conjugation at one end of the C=C double bond. The similar p-π conjugation could be found in both of the two reactants (shown in Table 1(a)) in this work. Therefore, in the present work, we only focus on the reaction pathway leading to the trans and cis cyclobutane products with carbonyls in ortho position (see Table 1(a)). All the energies used in the discussion are the free energies in the solvent unless otherwise noted.

3.1 Formation of radical anions

According to our previous studies on the intermolecular cycloaddition of phenyl vinyl sulfone with enone,[21] the crucial step of the cycloaddition is the formation of the radical anion. In the cycloaddition of enones, the experimentalists used the aryl enone to afford the radical anion.[15] However, considering that the electron-accepting ability is strongly influenced by the substituents, it is necessary to measure the molecule's electron-accepting ability by calculating the adiabatic electron affinities (EA_{ad}) of the reactants.

As shown in Table 2, the order of the EA_{ad} in solvent is the same to that in gas phase, but the EA_{ad} values in solvent are considerably lower than those in gas phase, indicating that the radical anion could be stabilized by the solvent. The order of the calculated EA_{ad} values is **R1d > R1b > R1a > R1c > R1e,** which is consistent with the electron-withdrawing capacity of the substituents: NO_2Ph > ClPh > Ph > MeOPh > NH_2Ph. Thus, strong electron-withdrawing substituents are beneficial for the formation of radical anion reactant. It is noted that the EA_{ad} value of **R1e** is the lowest, indicating the disadvantage for **R1e** to afford the radical anion over other reactants. Similarly, the EA_{ad} of **R2d** and **R2f** with electron-withdrawing substituents

are much larger than those of **R2a**, **R2b**, **R2c** and **R2e** with electron-donating substituents. In the cycloadditions of **R1(a-g)** and **R2a**, as the EA_{ad} values of **R1(a-g)** are all larger than that of **R2a**, the formed radial anions should be **R1(a-g)**$^{\bullet-}$. It is noted that, in the cycloadditions of **R1a** and **R2(a-c, e)**, the formed radical anion should be **R1a**$^{\bullet-}$, while in the cycloadditions of **R1a** and **R2(d,f)**, the formed radical anions should be **R2(d,f)**$^{\bullet-}$. The above analysis shows that in reactions 1-3 and 6-9, the radical anions are formed by the aryl enones indeed, which confirms the prediction by the experimentalist.

3.2 Analysis of the global electronic indexes of the reactants

After the two reactants for the cycloaddition are determined, it is necessary to explore the reactivity of the reactants before discussing the reaction profiles. Since the global electronic indexes are useful tools to understand the reactivity of molecules in their ground states,[33] we calculated the chemical potential μ, chemical hardness η, global electrophilicity ω and the maximum amount of electronic charge ΔN_{max} (see Table 3) to analyze the nature of interaction between the two reactants of the cycloaddition. The indexes μ and η are defined as[34] $\mu \approx \frac{\varepsilon_H + \varepsilon_L}{2}$ and $\eta \approx \varepsilon_L - \varepsilon_H$, respectively, where the ε_H is the energy of the highest occupied orbital, and ε_L is the energy of the lowest unoccupied orbital. The global electrophilicity ω, which measures the stabilization in energy when the system acquires an additional electronic charge ΔN from the environment, is given by the simple expression[35]: $\omega = \frac{\mu^2}{2\eta}$. The maximum amount of electronic charge that the electrophile system may accept is given by[35] $\Delta N_{max} = -\frac{\mu}{\eta}$.

As shown in Table 3, according to the scale proposed by Domingo et al,[36] the radical anion reactants are moderate electrophiles except those with strong electron-withdrawing substituents which can be considered as nucleophiles (marginal

electrophiles). The neutral reactants are all strong electrophiles. The maximum charges ΔN_{max} of the neutral reactants are positive, and the values decrease with the global electrophilicity, which is consistent with the previous work[36]. The radical anion reactants are all negative, indicating that the electron may transfer from the radical anion towards the environment. However, the trend that the absolute values decrease with the global electrophilicity is conserved. Since the two reactants are classified as a strong and a moderate electrophile or a strong and a marginal electrophile, respectively, the [2+2] cycloaddition will present a charge transfer pattern. The chemical potential of the neutral reactants are lower than that of the radical anion reactants, indicating that the charge will take place from the radical anion towards the neutral reactants. To evaluate this charge transfer, we calculated the index ΔN^0 according to the formula[37]: $\Delta N^0 = (\mu_1 - \mu_2)/(\eta_1 + \eta_2)$. As shown in Table 4, the value of ΔN^0 also confirms the charge transfer from the radical anion towards the neutral reactants. The large difference in electrophilicity ($\Delta\omega$) within the two reactants (see Table 4) suggests the polar character of the cycloaddition, which is consistent with the charge transfer analysis.

3.3 Mechanisms of the cycloaddition reactions

As we described above, the [2+2] cycloaddition proceeds stepwise between the radical anion and the neutral molecule, involving the breakage of two π bonds and the formation of two σ bonds. We collected the main geometrical (bond lengths of the two forming σ bonds, indexes of bond advancement) and electronic parameters (dipole moments, charge transfer indexes) [38] of the critical structures for the reactions 1-16 in Table S1 (see the Supporting Information). Along the reaction pathway, the first step of the cycloaddition is the formation of a pre-reaction complex (**PC**) corresponding to the local minimum. According to the lengths of C1-C3 and C2-C4 (see the definitions in Fig. 2) bonds and the indexes of bond advancement, the formation of C1-C3 bond has the priority to the formation of C2-C4 bond in the cyclization reaction, since the C1-C3 distance is significantly shorter than the C2-C4

distance in **PCs** (see Table S1). In reactions 1-3, 5, 6, 8, 9 and 13-16, the **PCs** have the similar structures to the corresponding first transition states (**TS1s**), where the difference in distance of C1-C3 between **PC** and **TS1** is shorter than 1.6 Å for each reaction, indicating that these **PCs** have properties of the orientation complex.[39,40] However, in reactions 4, 7 and 10-12, the **PCs** do not show the spatial orientations observed in the **TS1s**, where the difference in distance of C1-C3 between **PC** and **TS1** is longer than 2.3 Å for each reaction. Actually, the two atoms which have the shortest distance in those **PCs** are O and H atoms. These O-H distances are all shorter than 2.2 Å; the angles of ∠O-H-C in **PC-4**, **PC-7**, **PC-10**, **PC-12** and ∠O-H-N in **PC-11** are almost 180°. Therefore, the formation of these **PCs** may be determined by the hydrogen bond interaction. As shown in Table S1, the charge transfer indexes suggest that the **PCs** except those with nitryl are charge transfer complexes, where the strong electron-withdrawing substituent may lead to that the electron is hard to transfer to the neutral molecule. An acyclic intermediate (**IM**) is formed via the transition state (**TS1**). For that the C1-C2 and C3-C4 bonds have been changed into single bonds, which could rotate freely to form the trans and cis products (**P-trans, P-cis**) via the respective transition states. The cycloadditions are polar, confirmed by the values of dipole moments and charge transfer indexes, which is in agreement with the above speculation of the polar cycloaddition based on the $\Delta\omega$ values.

The relative free energies of the main structures along reactions 1-16 are shown in Table 5. Take reaction 1 for instance, as shown in the potential energy profile (see Fig. 1), the formation of **PC-1** is associated with a slight decrease of the enthalpy and a positive relative free energy in gas phase, indicating the impossibility as stable intermediate. According to our calculational results, the **PC-1** valley in the energy profiles disappears in the solvent, and the activation barriers are also decreased by the solvent (see Tables 5 and S2). We use **PC-1** as the start of the cycloaddition and the free energies in solvent at 298 K to discuss the reaction process. From **PC-1**, the activation barrier to form the acyclic intermediate **IM-1** is predicted to be 3.2 kcal/mol. The **TS1-1** and **IM-1** are all polar, confirmed by the dipole moments ($\mu >$

4D) and charge transfer indexes (t=0.43e, t=0.52e) shown in Table S1. Subsequently, there is a bifurcation from **IM-1**, which leads to the trans product with lower polarity and cis product with higher polarity, respectively. The charge transfer indexes show that the charge transfer increased in the second transition states and decreased when the products are formed. The activation barrier to form **P-trans-1** is 3.8 kcal/mol, and the activation barrier to form **P-cis-1** is 6.8 kcal/mol. It is obvious that the barrier to form **P-cis-1** is much higher than that to form **P-trans-1**, indicating that the reaction pathway to form **P-trans-1** is more dynamically favorable. Additionally, **P-trans-1** is more thermodynamically stable than **P-cis-1**. Therefore, the cycloaddition to form **P-trans-1** has an absolute advantage over that to form **P-cis-1**, which is in agreement with the experimental result that **P-trans-1** is the mainly observed product for the cycloaddition of **R1a** and **R2a**. The cycloaddition processes of the rest reactions 2-16 are analogous to that of reaction 1. Thus, we won't discuss these processes in detail again. Considering that the relative free energies of **TS2-trans** are lower than those of **TS1** for all the reactions, we only use the free energy of **TS1** to discuss the reactivity of the cycloaddition in the following.

3.4 Substituent effects on the reactivity

3.4.1 Influence of electronic structures on the reactivity

The experimental result shows that both electron-withdrawing and electron-donating substituents (reactions 1-3) are amenable to cycloaddition. However, whether the strong electron-withdrawing and electron-donating substituents are amenable to cycloaddition is unknown. Therefore, we designed reactions 4-5 and 10 to investigate the effect of the strong electron-withdrawing and electron-donating substituents on the cycloaddition. To discuss the electronic structure effect of the substituents at the two dissimilar enones on the cycloaddition, we divided the reactions into two groups. One group includes reactions 1-5 with different substituents at R^1-position; the other includes reactions 9 and 10 with different substituents at R^3-position (see notations in Table 1(a)).

As shown in Table 5, the first activation barriers of reactions 1-3 and 5 are 3.2, 5.8, 2.7 and 2.2 kcal/mol, respectively; the second activation barriers to form the trans

products are no more than 4.9 kcal/mol. The moderate activation barriers indicate that both electron-withdrawing and electron-donating substituted enones could undergo cycloadditions. However, the first activation barrier of reaction 4 with nitryl on the phenyl is predicted to be 22.1 kcal/mol, which is 18.9 kcal/mol higher than that of reaction 1, indicating that too strong electron-withdrawing is unfavorable for the cycloaddition. Considering that all the stereo structures along these reactions are similar, the difference in reactivity must be caused by the electronic effect. It is subjected to further investigation into the electronic structures. Therefore, we performed NBO calculations to get the NBO charges on the moiety of the key structures.

As we have declared in our previous investigation for the intramolecular cycloaddition of bis(enone),[19] the cycloaddition reactivity is influenced by the charges on the reaction centre (**RC**) including C1, C2, C3 and C4 atoms (see notations in Fig. 2). We only present the NBO charges on these four atoms in this work. As shown in Table 6, the NBO charges on **RC** of the key structures are almost -1 e, suggesting that the additional electron mainly focuses on the reaction centre along the cycloaddition.

The additional negative charges on **RC** should be advantageous for the first step of the cycloaddition, as the electron on the π* antibonding orbital could weaken the C=C bond. This is confirmed by the calculational results that the reaction with a more negative **RC** would have the lower first activation barrier. As shown in Table 6, the NBO charges on **RC** are strongly affected by the electronic structure of the substituents. The electron-donating substituent is helpful for the formation of a more negative **RC**, which is beneficial for the first step of the cycloaddition. Thereby, the electron-withdrawing substituent would increase the first activation barrier. However, according to the relationship between the NBO charges on **RC** and the first activation barrier, the first activation barrier of reaction 4 should not be so significantly high as the NBO charges on **RC** in **TS1-4** are not dramatic decreased. By comparing the distribution of the NBO charges we find that the Coulombic repulsion between C1 and C3 also has effect on the first activation barrier. The NBO analysis shows that the Coulombic repulsion between C1 and C3 in **TS1-2** is the smallest and that in **TS1-4** is

the largest among **TS1-1** to **TS1-5**, making the energy of **TS1-2** decrease and the energy of **TS1-4** increase. Therefore, although the difference in NBO charges on **RC** between **TS1-2** and **TS1-4** is not considerable, the first activation barrier of reaction 2 is moderate, while that of reaction 4 is significantly high.

After the C1-C3 bond is formed, the NBO charges on C1 and C3 atoms increase, and the NBO charges on C2 and C4 atoms decrease, which is favorable for weakening the Coulombic repulsion between C2 and C4, benefiting the formation of C2-C4 bond. In the second cycloaddition step, the NBO charges on **RC** are decreased. The reaction 4, with less negative NBO charges on **RC** and weak Coulombic repulsion between C2 and C4 in the second transition states, has the lowest second activation barrier comparing to reactions 1-3 and 5, indicating that the electron-withdrawing substituent is beneficial for the second cycloaddition step.

To investigate the electronic effect of the reacting partner on the cycloaddition, we also performed NBO analysis on the key structures of reactions 9 and 10 with methoxyl and nitryl substituents at R^3-position. The effect of the methoxyl on **RC** is strong, as the NBO charges on **RC** in **TS1-9** are the most negative shown in Table 6. With the increasing of the charges on **RC**, the NBO charges on C1 and C3 become more negative as well, leading to the stronger Coulombic repulsion between C1 and C3. Therefore, although the NBO charges on **RC** in **TS1-9** are more negative than those in **TS1-1**, the first activation barrier of reaction 9 is 3.6 kcal/mol higher. The NBO charges on **RC** in **TS1-10** are a little less negative than those in **TS1-1** caused by the effect of the nitryl at R^3-position. However, this insignificant effect on the NBO charges on **RC** could not explain the significant higher in the free energy of **TS1-10** than **TS1-1**. Then, we check the structure of **TS1-10** and find that the C-N bond is 1.61 Å, which is much longer than that in **PC-10** (1.45 Å). The elongation of the C-N bond may be caused by the increasing Coulombic repulsion between the C and N atoms, as the NBO charges on C and N atoms in **TS1-10** are 0.525 and 0.418 e, which are more positive than those in **PC-10** (0.498 e, 0.342 e). This strong Coulombic repulsion weakens the C-N σ bond interaction, increasing the energy of **TS1-10**.

In conclusion, the first cycloaddition step needs a more negative **RC**, while the second cycloaddition step needs a less negative **RC**. Both of the electron-donating and electron-withdrawing substituents are amenable to cycloaddition, which is consistent with the experimental result. However, too strong electron-withdrawing substituents at either of the two dissimilar enones significantly increase the first activation barrier, indicating that the nitryl is unfavorable for the cycloaddition. This conclusion confirms our previous conjecture in the investigation of the bis(enones) again.[19]

3.4.2 Influence of steric hindrance on the reactivity

Since the first step of the cycloaddition is the formation of the C1-C3 σ bond, the steric hindrance on C1 and C3 should have effect on the reactivity of the cycloaddition. Therefore, we investigated reactions 6-8, which have more bulky substituents at R^2- and R^4-position. In reaction 6, the ethyl is used to instead of methyl on C1 in reaction 1. The first activation barrier of reaction 6 is 1.2 kcal/mol higher than that of reaction 1. When the substituents on C1 changes into tert-butyl, the first activation barrier of reaction 7 is 10.2 kcal/mol higher than that of reaction 1, indicating that the first activation barrier of the cycloaddition is strongly influenced by the increasing size of the substituents on C1. When there are methyl substituents on both of C1 and C3 atoms, the increased steric hindrance leads to that the first activation barrier of reaction 8 is 7.7 kcal/mol higher than that of reaction 1, which confirms the experimental result that the reactivity of the cycloaddition is sensitive to the substituents on C3 atom. The steric hindrance also increases the relative energies of **IM-(6-8)**, which is 2.3, 2.4 and 8.6 kcal/mol higher than that of **IM-1**, respectively. However, the second transition states are not affected by the steric hindrance on C1 and C3 too much. Thus, the second activation barriers of reaction 6-8 are decreased and lower than that of reaction 1.

As we talked above, the cycloaddition is sensitive to the steric bulk at R^2- and R^4-position, but the methyl is amenable. Considering that the R^2-position is equal to the R^4-position in influencing the cycloaddition, we only change the substituents at R^4-position to discuss the effect on the reaction reactivity. In order to check the

possibility of constructing other full-substituted cyclobutanes by the radical anion cycloaddition, we tried to add the amino and nitryl to the R^4-position. As shown in Table 5, the first activation barriers of reactions 11 and 12 are significantly higher than that of reaction 1, which should be caused by both of the electronic effect and steric effect. Considering that the steric hindrance caused by the amino and nitryl has no big difference to the methyl, the energy difference between **TS1-(11, 12)** and **TS1-8** should be attributed to the electronic effect.

The NBO charges on **RC** in **TS1-11** and **TS1-12** are -0.901 and -0.936 e, respectively, which are considerably less negative than the reactions shown in Table 6, explaining the significant high first activation barriers of reactions 11 and 12. Specially, the NBO charges on C3 in **TS1-11** and **TS1-12** are 0.015 and -0.080 e, respectively, notably influenced by the substituents on C3 atom, while those on C1 atom are -0.198 and -0.101 e, respectively. The stronger Coulombic repulsion between C1 and C3 in **TS1-12** may just explain why the relative free energy of **TS1-12** is 4.6 kcal/mol higher than that of **TS1-11**. For that the energy difference between **TS1-(11, 12)** and **TS1-8** is similar to that between **TS1-8** and **TS1-1**, the contribution of electronic effect and steric effect on the reaction reactivity should be equivalent.

Additionally, it should be mentioned that the relative free energy of **PC-11** are considerably lower than those in other reactions, which is caused by the formation of the hydrogen bond between the H atom of amino and the O atom of carbonyl in the complexes as we talked above. The stabilization of the complex is unfavorable for the cycloaddition, since it will need more energy to break the hydrogen bond and undergo the following reaction.

3.5 Substituent effects on the chemoselectivity

As mentioned above, the reactions 1-3, 6, 7 and 9 all have excellent chemoselectivity, giving the crossed [2+2] cycloaddition product as domination. However, in the reaction of **R1a** and **R2b** (reaction 8), **R1a** undergoes the [2+2] cycloaddition not only with **R2b**, but also with itself. And the yield of the homodimer of **R1a** is even larger than that of the crossed cycloaddition product. To understand the origin of the chemoselectivity, we compared the activation barriers of the crossed and

self [2+2] cycloadditions.

As shown in Table 5, the fist activation barriers for the crossed cycloadditions (reactions 1,2, 3, 6 and 9) are 3.2, 5.8, 2.7, 4.3 and 6.8 kcal/mol, respectively; the fist activation barriers for the corresponding self cycloadditions (reactions 13, 14, 15, 16 and 13) are 7.4, 7.2, 7.7, 8.4 and 7.4 kcal/mol, respectively. The first activation barriers of the crossed cycloaddition above are all lower than their corresponding self cycloadditions, indicating the chemoselectivity to form the crossed cycloaddition products as the main product. As we talked above, the first activation barrier is strongly affected by the steric hindrance at R^2- and R^4-position. This well explains the predomination of the crossed cycloaddition with substituents only at R^2-position over the self cycloaddition with substituents at both of R^2- and R^4-positions. Therefore, considering the bulky substituents at R^2-position in **R1g**, the self cycloaddition of **R1g** should be extremely unfavorable.

The first activation barrier of reaction 8 is 0.8 kcal/mol higher than that of reaction 13, suggesting the self cycloaddition of **R1a** has slight advantage over its crossed cycloaddition with **R2b**, which is in agreement with the experimental result. It is obvious that the difference of the steric hindrance in the first step of these two reactions is ignorable. Thus, we tried to explain the predomination of the self cycloaddition from the NBO analysis. However, the NBO charges on **RC** in **TS1-8** are more negative than those in **TS1-13**, which indicates that the relative free energy of **TS1-8** even should be lower than that of **TS1-13**. Nonetheless, the important feature of **TS1-13**, that is the strong conjugation effect caused by the two existing phenyl substituents, may contribute to reduce the energy of **TS1-13**. Although the chemoselectivity is not good as the difference in the first activation barrier between reactions 8 and 13 is small, the stereoselectivity for each cycloaddition is still excellent, which will be discussed in the following part.

3.6 The origin of the stereoselectivity

As shown in Table 5, the energies of the trans second transition states and products are all lower than those of the corresponding cis second transition states and products respectively, indicating that the reaction pathway to form the trans product is both dynamically and thermodynamically favorable, showing the good stereoselectivity. The electronic and steric effect of the substituents on the

stereoselectivity is discussed in detail below.

According to the NBO charges displayed in Table 6, the NBO charges on **RC** in **TS2-trans** are less negative than those in **TS2-cis**. As we talked above, the less negative **RC** is beneficial for the second cycloaddition step, suggesting that the energy of **TS2-trans** should be lower than that of **TS2-cis**. Additionally, the Coulombic repulsion between C2 and C4 in **TS2-trans** is a little weaker than that in **TS2-cis**, which also contributes to reduce the energy of **TS2-trans**. However, the energy difference between the **TS2-trans** and **TS2-cis** changes slightly for reactions 1-5 with significant different electronic structures, indicating that the electronic effect on the stereoselectivity is restricted. Thus, we predict that the stereoselectivity is primarily influenced by the steric hindrance.

As shown in Fig. 2, in **TS2-cis-1**, the carbonyl substituents on C2 and C4 are in the same side. The distance between the two O atoms is 4.10Å, showing the stronger steric interaction. While in **TS2-trans-1**, the carbonyl substituents on C2 and C4 are in the different side. The distance between the two O atoms is 5.64 Å, showing the weaker steric interaction. The difference in steric interactions contributes to the excellent stereoselectivity. The experimental results show that the stereoselectivity of reaction 9 is not so excellent as other reactions (reactions 1-3 and 6-8), which is confirmed by our calculational result that the energy difference between **TS2-trans-9** and **TS2-cis-9** is smaller than that in reactions 1-3 and 6-8. To understand the origin of the unusual stereoselectivity, we herein examine the structures of diastereomeric **TS2-trans-9** and **TS2-cis-9** (Fig. 2). In **TS2-trans-9**, although the steric hindrance between the carbonyl substituents on C2 and C4 are weaker than that in **TS2-cis-9**, the steric hindrance between the phenyl and the methyl on O atom is much stronger than that in **TS2-cis-9**. The cooperation of these two factors decreases the energy difference between **TS2-trans-9** and **TS2-cis-9**. Therefore, the stereoselectivity of reaction 9 is not excellent.

The reason causing the decrease of the energy difference between **TS2-trans-4** and **TS2-cis-4** is analogous to that in reaction 9. Furthermore, the distances between C2 and C4 in **TS2-trans-4** and **TS2-cis-4** are the longest among those in all reactions,

suggesting that the steric effect on the stereoselectivity of reaction 4 becomes weak. This could explain that the energy difference between **TS2-trans-4** and **TS2-cis-4** is smaller than that in reaction 9. The energy of **TS2-trans-10** is 2.1 kcal/mol lower than that of **TS2-cis-10**, which is little smaller than the energy difference between **TS2-trans-9** and **TS2-cis-9,** indicating that the stereoselectivity is not good either. The distance between the H atom on phenyl and the O atom on nitryl in **TS2-cis-10** is shorter than that in **TS2-trans-10**, indicating the stronger Coulombic attraction between the H and O atoms in **TS2-cis-10**. Thus, the energy difference between **TS2-trans-10** and **TS2-cis-10** is decreased, which is unfavorable for keeping the stereoselectivity.

The reaction 8 with ethyl R^3-position is predicted to demonstrate excellent stereoselectivity since the **TS2-trans-8** is favored by 5.8 kcal/mol to **TS2-cis-8**. It is interesting to discover the similar improving trend in stereoselectivity in reaction 13-16 substituted by phenyl at R^3-position, where the **TS2-trans-(13-16)** is 6.5, 6.4, 7.3 and 6.6 kcal/mol lower in free energy than **TS2-cis-(13-16),** respectively. The origin of much lower energies of **TS2-trans-(13-16)** can be understood on the basis of the strong steric interaction between the two phenyl substituents in the cis structure. Therefore, we can speculate that the steric hindrance at R^1- and R^3-positions could increase the energy difference between the trans and cis transition states. To improve the stereoselectivity, it is better to introduce bulky substituents at R^1- and R^3-positions.

4. Conclusion

In summary, we have presented a detailed DFT study on the substituent effect on the chemo- and stereoselectivity of the crossed intermolecular radical anion cycloadditions of various enones. The cycloaddition process is stepwise with the polar nature, for which the more negative **RC** is favorable for the first step; the less negative **RC** is favorable for the second step. However, too strong electron-withdrawing substituents will significantly increase the first activation barrier, suggesting that nitryl should not be introduced to the radical anion cycloaddition.

The cycloaddition is sensitive to the substituents at R^2- and R^4-positions by both

steric hindrance and electronic effect. To improve the chemoselectivity, it is better to keep the R^4-position unsubstituted. The stereoselectivity is mainly caused by the steric hindrance, and the electronic effect only has slight influence on the stereoselectivity. Therefore, in order to improve the stereoselectivity, it is better to introduce bulky substituents at R^1- and R^3-positions to increase the difference in steric interaction between the trans and cis transition states.

Our investigation shows that the electronic and stereo structures of the substituents have dramatic effect on the radical anion cycloadditions. Especially, the amino and nitryl could be hardly endured. This work provides useful information for choosing substituents to design novel intermolecular [2+2] cycloadditions with excellent chemo- and stereoselectivity.

Acknowlegement

We gratefully acknowledge the National Natural Science Foundation of China (No.21373217 and No.21173262) for supporting this work.

References

[1] T. V. Hansen, Y. Stenstrøm, Naturally Occurring Cyclobutanes in Organic Synthesis: Theory and Applications, Elsevier, Oxford, U.K., 2001, vol. 5, pp.1-38.

[2] V. M. Dembitsky, J. Nat. Med., 2008, **62**, 1-33.

[3] M. T. Crimmins, Chem. Rev., 1988, **88**, 1453-1473.

[4] J. D. Winkel, at al., Chem. Rev., 1995, **95**, 2003-2020.

[5] D. J. Schuster, et al., Chem. Rev., 1993, **93**, 3-22.

[6] J. Iriondo-Alberdi, M. F. Greaney, Eur. J. Org. Chem., 2007, **29**, 4801-4815.

[7] N. Hoffmann. Chem. Rev., 2008, **108**, 1052-1103.

[8] N. L. Bauld, R. Pabon, J. Am. Chem. Soc., 1983, **105**, 633-634.

[9] N.P. Schepp, L. J. Johnston, J. Am. Chem. Soc., 1996, **118**, 2872-2881.

[10] N. P. Schepp, D. Shukla, H. Sarker, N. L. Bauld, L. J. Johnston, J. Am. Chem. Soc., 1997, **119**, 10325-10334.

[11] Y. Okada, R. Akaba, K Chiba, Org. Lett., 2009, **11**, 1033-1035.

[12] G. A. N. Fetton, N. L. Bauld, Tetrahedron Letters., 2004, **45**, 8465-8469.

[13] J. Yang, Gre A. N. Felton, N. L. Bauld, J. Am. Chem. Soc., 2004, **126**, 1634-1635.

[14] M. A. Ischay, M. E. Anzovino, J. Du, T. P. Yoon, J. Am. Chem. Soc., 2008, **130**, 12886-12887.

[15] J. Du, T. P. Yoon, J. Am. Chem. Soc., 2009, **131**, 14604-14605.

[16] M. A. Ischay, Z. Lu, T. P. Yoon, J. Am. Chem. Soc., 2010, **132**, 8572-8574.

[17] M. A. Ischay, M. S. Ament, T. P. Yoon, J. Am. Chem. Soc., 2012, **3**, 2807-2811.

[18] Q. Zhang, Z. Li, B. Chen, Comput. Theor. Chem., 2009, **901**, 202-209.

[19] J. Yuan, Q. Zhang, B. Chen, Comput. Theor. Chem., 2012, **996**, 110-116.

[20] C. Guo, L. Cui, B. Chen, J. Yuan, Z. Tian, RSC Adv., 2012, **2**, 9932-9937.

[21] C. Guo, J. Yuan, B. Chen, Z. Tian, Comput. Theor. Chem., 2014, **1028**, 27-33.

[22] A. D. Becke. J. Chem. Phys., 1993, **98**, 5648-5653.

[23] C. Lee, W. Yang, R. G. Parr, Phys. Rev. B., 1988, **37**, 785-789.

[24] S. H. Vosko, L. Wilk, M. Nusair, Can. J. Phys. 1980, **58**, 1200-1211.

[25] Y. Zhao, D.G. Truhlar, Accounts Chem. Res., 2008, **41**, 157-167.

[26] K. Fukui, Accounts Chem. Res., 1981, **14**, 363-368.

[27] C. Gonzalez, H.B. Schlegel, J. Chem. Phys., 1989, **90**, 2154-2162.

[28] C. Gonzalez, H.B. Schlegel, J. Phys. Chem. 1990, **94**, 5523-5527.

[29] M. J. Frisch, G. W. Trucks, H. B. Schlegel, G. E. Scuseria, M. A. Robb, J. R. Cheeseman, V. G. Zakrzewski, J. A. Montgomery, R. E. Stratmann, J. C. Burant, S. Dapprich, J. M. Millam, A. D. Daniels, K. N. Kudin, M. C. Strain, O. Farkas, J. Tomasi, V. Barone, M. Cossi, R. Cammi, B. Mennucci, C. Pomelli, C. Adamo, S. Clifford, J. Ochterski, G. A. Petersson, P.Y. Ayala, Q. Cui, K. Morokuma, A. D. Malick, K. D. Rabuck, K. Raghavachari, J. B. Foresman, J. Cioslowski, J. V. Ortiz, A. G. Baboul, B. B. Stefanov, G. Liu, A. Liashenko, P. Piskorz, I.

Komaromi, R. Gomperts, R. L. Martin, D. J. Fox, T. Keith, M. A. Al-Laham, C. Y. Peng, A. Nanayakkara, M. Challacombe, P. M.W. Gill, B. Johnson, W. Chen, M. W. Wong, J. L. Andres, C. Gonzalez, M. Head-Gordon, E. S. Replogle, J. A. Pople, Gaussian 09, G. I. Revision A. 1-SMP, Wallingford, CT (2009).

[30] A. V. Marenich, C. J. Cramer, D. G. Truhlar. J. Phys. Chem. B., 2009, **113**, 6378-6396.

[31] Q. S. Li, R. H. Lü, Y. M. Xie, H. F. Schaefer, J. Comput. Chem., 2002, **23**, 1642-1655.

[32] A. Elkechai, A. Boucekkine, L. Belkhiri, M. H. Amarouche, C. Clappe, D. Hauchardf, M. Ephritikhineg, Dalton Trans., 2009, **15**, 2843-2849.

[33] P. K. Chattaraj, S.Giri, S. Duley, Chem. Rev.,2011, **111**, PR3-PR47.

[34] R. G. Parr, W. Yang, Densitiy Funcional Theory of Atoms and Molecules, Oxfrd University : New York, 1989.

[35] R. G. Parr, L. Szentpaly, S. Liu, J. Am. Chem. Soc., 1999, **121**, 1922-1924.

[36] L. R. Domingo, M. J. Aurell, P. Pérez, R. Contreras, Terahedron, 2002, **58**, 4417-4423.

[37] R. G. Parr, R. G. Pearson, J. Am. Chem. Soc., 1983, **105**, 7512- 7516.

[38] R. Jasiński, A. Barański, J. Mol. Struct : Theo Chem, 2010, 949, 8-13.

[39] R. Jasiński, Tetrahedron, 2013, **69**, 927-932.

[40] R. Jasiński, O. Koifman, A. Barański, Cent. Eur. J. Chem. 2011, **9**, 1008-118.

Table 1
Intermolecular radical anion cycloaddition reactions of various enones.

(a)

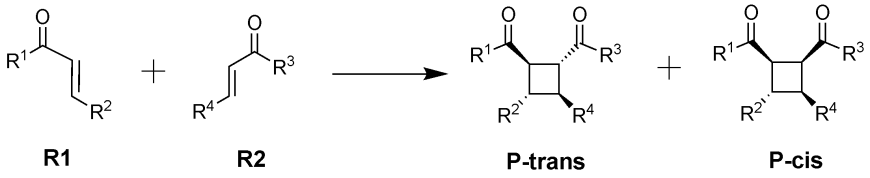

(b)

Reactions	R^1	R^2	R^3	R^4	Reactions	R^1	R^2	R^3	R^4
1 (**R1a+R2a**)	Ph	Me	Me	H	**9** (**R1a+R2c**)	Ph	Me	MeO	H
2 (**R1b+R2a**)	ClPh	Me	Me	H	**10** (**R1a+R2d**)	Ph	Me	NO_2	H
3 (**R1c+R2a**)	MeOPh	Me	Me	H	**11**(**R1a+R2e**)	Ph	Me	Me	NH_2
4 (**R1d+R2a**)	NO_2Ph	Me	Me	H	**12** (**R1a+R2f**)	Ph	Me	Me	NO_2
5 (**R1e+R2a**)	NH_2Ph	Me	Me	H	**13** (**R1a+R1a**)	Ph	Me	Ph	Me
6 (**R1f+R2a**)	Ph	Et	Me	H	**14** (**R1b+R1b**)	ClPh	Me	ClPh	Me
7(**R1g+R2a**)	Ph	*t*-Bu	Me	H	**15** (**R1c+R1c**)	MeOPh	Me	MeOPh	Me
8 (**R1a+R2b**)	Ph	Me	Et	Me	**16** (**R1f+R1f**)	Ph	Et	Ph	Et

Table 2
Adiabatic electron affinities (EA_{ad}) of all the reactants in gas phase and solvent calculated at B3LYP/6-311+G(d,p) level (including the ZPE corrections). All values are given in kcal/mol.

Species	**[a]EA_{ad}(Vacuum)**	**[a]EA_{ad}(CH_3CN)**	**Species**	**[a]EA_{ad}(Vacuum)**	**[a]EA_{ad}(CH_3CN)**
R1a	17.9	58.9	**R2a**	7.5	49.8
R1b	23.1	60.7	**R2b**	4.1	48.9
R1c	14.5	55.3	**R2c**	2.8	41.7
R1d	46.3	81.7	**R2d**	46.3	89.4
R1e	11.7	53.2	**R2e**	-6.9	38.2
R1f	18.8	59.1	**R2f**	50.8	134.5
R1g	16.2	56.9			

[a] EA_{ad} = *E*(optimized neutral) – *E*(optimized anion) [31,32]

Table 3
Global electrophilicity scale and global properities for the reactants in the [2+2] cycloaddition.

Species	ω [ev]	μ [a.u.]	η [a.u.]	ΔN_{max} [e]	Species	ω [ev]	μ [a.u.]	η [a.u.]	ΔN_{max} [e]
R1a$^{\bullet-}$	0.85	0.0679	0.0733	-0.9255	**R2a**	2.03	-0.1701	0.1847	0.9209
R1b$^{\bullet-}$	0.64	0.0611	0.0797	-0.7675	**R2b**	1.73	-0.1569	0.1939	0.8094
R1c$^{\bullet-}$	1.02	0.0618	0.0508	-1.2152	**R2c**	1.86	-0.1763	0.2274	0.7751
R1d$^{\bullet-}$	0.04	0.0154	0.0720	-0.2134	**R2d**$^{\bullet-}$	0.27	0.0457	0.1062	-0.4300
R1e$^{\bullet-}$	1.09	0.0641	0.0510	-1.2553	**R2e**	1.26	-0.1330	0.1914	0.6947
R1f$^{\bullet-}$	0.77	0.0619	0.0675	-0.9170	**R2f**$^{\bullet-}$	0.20	0.0438	0.1279	-0.3425
R1g$^{\bullet-}$	0.74	0.0577	0.0611	-0.9448	**R1a**	2.21	-0.1699	0.1780	0.9545

Table 4
The difference in electrophilicity power and the polarity values for the reactants of the [2+2] cycloaditions.

Reactions	$\Delta\omega$ [ev]	ΔN^0 [e]	Reactions	$\Delta\omega$ [ev]	ΔN^0 [e]
1 (R1a$^{\bullet-}$ +R2a)	1.18	0.90	**9 (R1a$^{\bullet-}$ +R2c)**	1.01	0.81
2 (R1b$^{\bullet-}$ +R2a)	1.39	0.85	**10 (R1a+ R2d$^{\bullet-}$)**	1.94	0.76
3 (R1c$^{\bullet-}$ +R2a)	1.01	0.96	**11 (R1a$^{\bullet-}$ +R2e)**	0.41	0.76
4 (R1d$^{\bullet-}$ +R2a)	1.99	0.70	**12 (R1a+ R2f$^{\bullet-}$)**	2.01	0.70
5 (R1e$^{\bullet-}$ +R2a)	0.94	0.96	**13 (R1a$^{\bullet-}$ +R1a)**	1.36	0.95
6 (R1f$^{\bullet-}$ +R2a)	1.26	0.89	**14 (R1b$^{\bullet-}$ +R1b)**	1.75	0.93
7 (R1g$^{\bullet-}$ +R2a)	1.29	0.90	**15 (R1c$^{\bullet-}$ +R1c)**	0.94	1.00
8 (R1a$^{\bullet-}$ +R2b)	0.88	0.84	**16 (R1f$^{\bullet-}$ +R1f)**	1.42	0.94

Table 5
The free energies at 298 K and 1 atm in solvent (CH_3CN) for the pre-reaction complexes, transition states, intermediates, and products along the cycloaddition pathways. The enthalpies at 298 K in gas phase are displayed in parentheses. All values are given in kcal/mol.

Reactions	R1+R2	PC	TS1	IM	TS2-trans	P-trans	TS2-cis	P-cis
1 (R1a+R2a)	0	0.8	4.0	-2.5	1.3	-5.2	4.3	-2.3
	(0)	(-7.2)	(-3.9)	(-9.0)	(-5.5)	(-10.6)	(-0.7)	(-6.5)
2 (R1b+R2a)	0	-0.8	5.0	-1.5	1.9	-5.7	4.8	-2.8
	(0)	(-6.4)	(-2.0)	(-7.1)	(-4.2)	(-10.4)	(0.6)	(-6.4)
3 (R1c+R2a)	0	-0.7	2.0	-4.5	0.1	-4.0	3.4	-1.0
	(0)	(-8.2)	(-5.4)	(-10.5)	(-6.6)	(-10.0)	(-1.5)	(-5.9)
4 (R1d+R2a)	0	-0.7	21.4	16.0	16.7	-9.5	18.6	-5.8
	(0)	(-4.5)	(12.0)	(8.7)	(8.8)	(-11.1)	(12.5)	(-7.5)
5 (R1e+R2a)	0	-1.0	1.2	-5.3	-0.4	-3.8	3.0	-0.7
	(0)	(-9.6)	(-6.3)	(-11.4)	(-7.2)	(-10.2)	(-2.1)	(-6.0)
6 (R1f+R2a)	0	1.6	5.9	-0.2	1.8	-4.9	4.8	-1.9
	(0)	(-5.9)	(-2.4)	(-7.2)	(-4.9)	(-10.0)	(0.0)	(-5.9)
7 (R1g+R2a)	0	-1.3	13.1	-0.1	3.0	-3.9	10.3	-0.9
	(0)	(-7.9)	(1.1)	(-2.9)	(-4.1)	(-9.3)	(0.9)	(-5.2)
8 (R1a+R2b)	0	1.9	12.8	6.1	7.5	1.9	13.3	9.0
	(0)	(-5.8)	(2.0)	(-3.6)	(-2.1)	(-6.4)	(4.7)	(1.8)
9 (R1a+R2c)	0	0.4	7.2	1.6	5.3	-4.0	7.5	-0.4
	(0)	(-6.5)	(-1.6)	(-5.7)	(-1.8)	(-7.0)	(2.5)	(-4.4)
10 (R1a+R2d)	0	0.1	18.6	10.4	16.1	-5.0	18.2	-3.5
	(0)	(-16.4)	(4.5)	(-0.5)	(5.7)	(-7.1)	(6.7)	(-4.0)
11 (R1a+R2e)	0	-6.4	21.2	17.8	17.8	11.0	20.0	14.6
	(0)	(-19.5)	(8.0)	(5.6)	(5.7)	(1.9)	(9.2)	(3.6)
12 (R1a+R2f)	0	0.0	25.7	22.5	23.8	16.6	29.3	23.5
	(0)	(-10.1)	(16.9)	(9.5)	(12.8)	(8.1)	(18.9)	(17.2)
13 (R1a+R1a)	0	3.5	10.9	1.9	3.6	-1.5	10.1	5.9
	(0)	(-8.9)	(-0.5)	(-7.4)	(-6.7)	(-12.2)	(1.7)	(-2.4)
14 (R1b+R1b)	0	3.3	10.5	1.4	3.6	-0.5	10.0	7.7
	(0)	(-9.1)	(-1.1)	(-8.1)	(-8.1)	(-14.0)	(0.2)	(-4.9)
15 (R1c+R1c)	0	3.4	11.1	2.1	2.2	-2.3	9.5	4.0
	(0)	(-7.3)	(0.1)	(-7.6)	(-6.6)	(-11.2)	(2.1)	(-0.8)
16 (R1f+R1f)	0	3.8	12.2	3.7	4.9	-0.4	11.5	7.1
	(0)	(-8.3)	(-0.3)	(-6.7)	(-6.5)	(-11.9)	(1.9)	(-2.5)

Table 6
NBO charges in e on the four C atoms for the main structures of the reactions 1-5, 9 and 10.

Reactions	atom	TS1	IM	TS2-trans	P-trans	TS2-cis	P-cis
1 (R1a+R2a)	C1	-0.177	-0.243	-0.249	-0.218	-0.253	-0.225
	C2	-0.342	-0.290	-0.221	-0.242	-0.220	-0.240
	C3	-0.345	-0.416	-0.393	-0.374	-0.394	-0.379
	C4	-0.389	-0.264	-0.298	-0.313	-0.306	-0.293
	RC	-1.253	-1.213	-1.161	-1.147	-1.173	-1.137
2 (R1b+R2a)	C1	-0.117	-0.240	-0.250	-0.216	-0.254	-0.223
	C2	-0.338	-0.299	-0.220	-0.242	-0.219	-0.241
	C3	-0.344	-0.419	-0.395	-0.373	-0.396	-0.379
	C4	-0.384	-0.249	-0.294	-0.312	-0.302	-0.293
	RC	-1.183	-1.207	-1.159	-1.143	-1.171	-1.136
3 (R1c+R2a)	C1	-0.175	-0.243	-0.246	-0.219	-0.251	-0.226
	C2	-0.351	-0.290	-0.226	-0.241	-0.225	-0.239
	C3	-0.348	0.415	-0.390	-0.374	-0.393	-0.380
	C4	-0.390	-0.270	-0.299	-0.312	-0.307	-0.294
	RC	-1.264	-1.218	-1.161	-1.146	-1.176	-1.139
4 (R1d+R2a)	C1	-0.190	-0.240	-0.260	-0.205	-0.265	-0.219
	C2	-0.281	-0.283	-0.227	-0.265	-0.221	-0.260
	C3	-0.349	-0.428	-0.413	-0.370	-0.412	-0.377
	C4	-0.345	-0.203	-0.237	-0.312	-0.246	-0.286
	RC	-1.165	-1.154	-1.137	-1.152	-1.144	-1.142
5 (R1e+R2a)	C1	-0.175	-0.244	-0.245	-0.219	-0.250	-0.226
	C2	-0.352	-0.286	-0.233	-0.241	-0.225	-0.230
	C3	-0.348	-0.413	-0.389	-0.375	-0.392	-0.380
	C4	-0.392	-0.279	-0.299	-0.311	-0.308	-0.294
	RC	-1.267	-1.222	-1.166	-1.146	-1.175	-1.130
9 (R1a+R2c)	C1	-0.190	-0.239	-0.253	-0.224	-0.256	-0.226
	C2	-0.340	-0.310	-0.222	-0.223	-0.216	-0.227
	C3	-0.349	-0.416	-0.389	-0.371	-0.389	-0.377
	C4	-0.408	-0.285	-0.329	-0.318	-0.335	-0.297
	RC	-1.287	-1.250	-1.193	-1.136	-1.196	-1.127
10 (R1a+R2d)	C1	-0.160	-0.262	-0.245	-0.209	-0.257	-0.222
	C2	-0.330	-0.187	-0.239	-0.285	-0.252	-0.292
	C3	-0.344	-0.385	-0.393	-0.372	-0.387	-0.353
	C4	-0.391	-0.366	-0.273	-0.270	-0.283	-0.291
	RC	-1.225	-1.200	-1.150	-1.136	-1.179	-1.158

Fig. 1

Free energy profiles for the reaction 1 leading to the stereoisomers. Enthalpies are displayed in parentheses. All the energies are given in kcal/mol in gas phase.

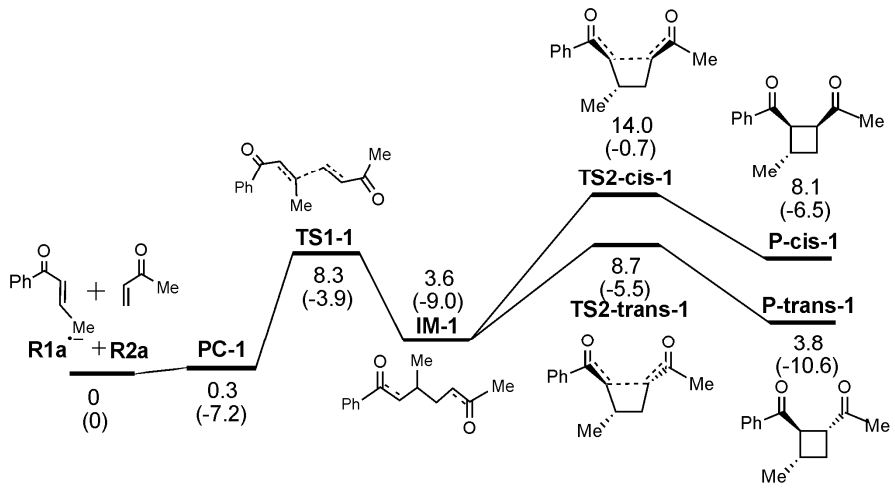

Fig. 2

Optimized geometries of the important transition states with selected bond distances given in angstrom.

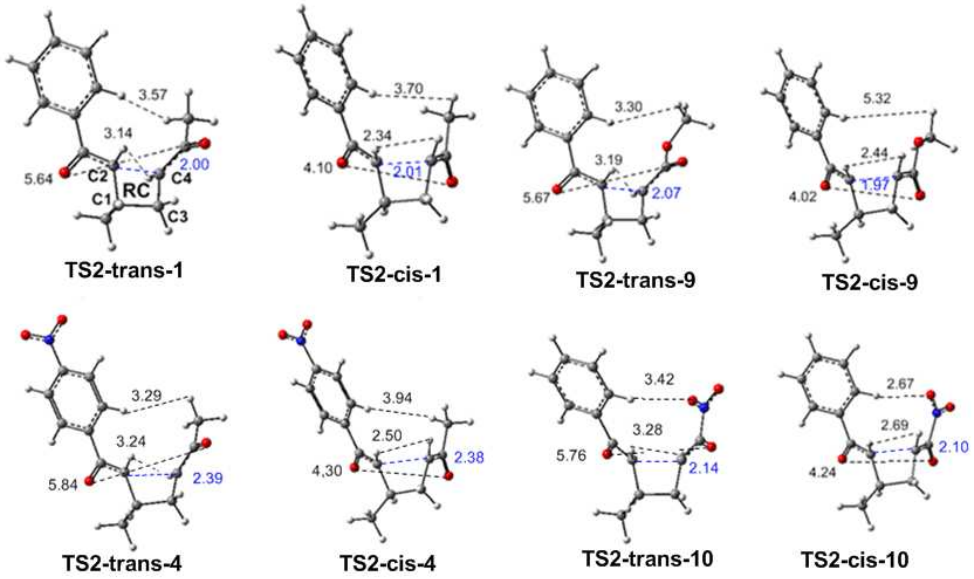

The chemoselectivity of cycloaddition is caused by the bulky group on the C atoms which form σ bond in the first cycloaddition step. The stereoselectivity mainly caused by the difference in steric interaction between the trans and cis transition states is benefited by the bulky substituents on the carbonyl.